metals

MDPI

Article

Effect of Hydrogen on the Elastic and Anelastic Properties of the R Phase in $Ti_{50}Ni_{46.1}Fe_{3.9}$ Alloy

Konstantin Sapozhnikov [1,2,*], Joan Torrens-Serra [3], Eduard Cesari [3], Jan Van Humbeeck [4] and Sergey Kustov [2,3]

1 Division of Solid State Physics, Ioffe Institute, Politekhnicheskaya 26, 194021 St. Petersburg, Russia
2 Department of Modern Functional Materials, ITMO University, Kronverkskiy 49, 197101 St. Petersburg, Russia; sergey.kustov@uib.es
3 Departament de Física, Universitat de les Illes Balears, Cra Valldemossa km 7.5, E 07122 Palma de Mallorca, Spain; j.torrens@uib.es (J.T.-S.); eduard.cesari@uib.cat (E.C.)
4 Departement Materiaalkunde (MTM), Katholieke Universiteit Leuven, Kasteelpark Arenberg 44, B-3001 Leuven, Belgium; jan.vanhumbeeck@kuleuven.be
* Correspondence: k.sapozhnikov@mail.ioffe.ru; Tel.: +7-812-2927119

Received: 12 October 2017; Accepted: 7 November 2017; Published: 10 November 2017

Abstract: The linear and non-linear internal friction, effective Young's modulus, and amplitude-dependent modulus defect of a $Ti_{50}Ni_{46.1}Fe_{3.9}$ alloy have been studied after different heat treatments, affecting hydrogen content, at temperatures of 13–300 K, and frequencies near 90 kHz. It has been shown that the contamination of the alloy by hydrogen gives rise to an internal friction maximum in the R martensitic phase and a complicated pinning stage in the temperature dependence of the effective Young's modulus at temperatures corresponding to the high-temperature side of the maximum. Dehydrogenation of the H-contaminated alloy transforms the internal friction maximum into a plateau and minimizes the pinning stage. The internal friction maximum is associated with a competition of two different temperature-dependent processes affecting the hydrogen concentration in the core regions of twin boundaries. The amplitude-dependent anelasticity of the R phase is also very sensitive to hydrogen content, its temperature dependence reflects the evolution of extended hydrogen atmospheres near twin boundaries.

Keywords: shape memory alloy; acoustic properties; internal friction; lattice defects; hydrogen

1. Introduction

Ti-Ni-based shape memory alloys are quite attractive functional materials [1]. Anelastic properties of Ti-Ni-based alloys are widely explored, both for microstructural characterization of the alloys and for their application as high-damping materials [2]. The effect of hydrogen on elastic and anelastic properties of Ti-Ni-based alloys have attracted considerable attention (see [3] for a review), especially after Fan et al. [4,5] have shown that hydrogen is unintentionally introduced during conventional heat treatment (water quenching after high-temperature annealing in argon-filled [4] or vacuum-sealed [5] quartz tubes) by the chemical reaction of residual water in quartz tubes with Ti at high temperatures. Fan et al. [4,5] have also shown that the relaxation internal friction (IF) peak observed by many researchers at low frequencies (about 200 K at 1 Hz) is due to an interaction of twin boundaries with hydrogen. Recently, we have studied the effect of hydrogen contamination during heat treatments on the low-temperature elastic and anelastic properties of a $Ni_{50.8}Ti_{49.2}$ alloy at ultrasonic frequencies, for which the '200 K' relaxation IF peak cannot be observed [6]. It has been shown that the hydrogen contamination gives rise to a non-relaxation internal IF maximum, whose temperature and height depend strongly on the hydrogen content. The IF maximum was interpreted as a pseudo-peak

formed due to a competition of two different temperature-dependent processes affecting the hydrogen concentration in the core regions of twin boundaries [6].

It seems important to check whether the new hydrogen-related anelastic effect, reported in [6], is inherent only in the B19′ martensitic phase, or it is common phenomenon for different martensitic phases of Ti-Ni-based alloys. The goal of the present work is to study the effect of hydrogen contamination on the elastic and anelastic properties of a Ti-Ni-based alloy with the R martensitic phase. The alloy composition was chosen in such a way that the B2↔R transformation type occurred, and the R martensitic phase could be tested over a wide temperature range. Such a situation takes place for $TiNi_{50-x}Fe_x$ alloys with $3 < x < 5$ [7]. Although there are data in the literature on the elastic and anelastic properties of Ti-$Ni_{50-x}Fe_x$ alloys [7–15], most of the data refer either to low x values, providing a narrow temperature range of the R phase, or to high ones, suppressing the martensitic transformation. Data for intermediate compositions are scarce and requires replenishment. The present paper is devoted to investigations of low-temperature elastic and anelastic properties of a $Ti_{50}Ni_{46.1}Fe_{3.9}$ alloy after two distinct heat treatments: conventional heat treatment contaminating the alloy by hydrogen and dehydrogenation treatment.

2. Materials and Methods

The $Ti_{50}Ni_{46.1}Fe_{3.9}$ alloy was prepared by induction melting of 99.99 wt. % pure components. Rod-shaped samples for acoustic and resistivity measurements were spark cut and mechanically polished. Two different heat treatments were used: (1) water quenching (WQ), (2) vacuum annealing (VA). The WQ treatment included annealing for 2 h at 1273 K in a vacuum-sealed quartz tube followed by quenching into water with breaking the tube. The VA treatment consisted in annealing for 26 h at 950 K under a residual gas pressure P $\approx 10^{-3}$ Pa. The annealing temperature was chosen to be higher than the temperature ranges of hydrogen desorption from Ni-Ti alloys reported in the literature [16–18]. Two samples were used for acoustic measurements: one after only the WQ treatment and another one subjected to a combination of the WQ and VA treatments.

The IF and effective Young's modulus, E, of the samples were measured at temperatures of 13–300 K by means of the resonant piezoelectric composite oscillator technique [19] using longitudinal oscillations at frequencies near 90 kHz. The logarithmic decrement δ, defined as $\delta = \Delta W/2W$, where ΔW is the energy dissipated per cycle and W is the maximum stored vibrational energy, was used as a measure of the IF. A computer-controlled setup [20] enabled us to measure quasi-simultaneously temperature dependences of the IF and Young's modulus at two values of oscillatory strain amplitude. At a low value of strain amplitude (10^{-6}), we monitored the linear (strain amplitude-independent) behaviour of the IF and Young's modulus. The non-linear (strain amplitude-dependent) effects were observed at a high value of strain amplitude (5×10^{-5}). The amplitude-dependent parts of the IF and Young's modulus defect, δ_h and $(\Delta E/E)_h$, were routinely derived from the differences of the IF and Young's modulus values registered at high and low strain amplitudes: $\delta_h = \delta(\varepsilon_m) - \delta_i$ and $(\Delta E/E)_h = (E_i - E(\varepsilon_m))/E_i$, where ε_m is the oscillatory strain amplitude, $\delta(\varepsilon_m)$, δ_i and $E(\varepsilon_m)$, E_i, are the values of the IF and Young's modulus in the amplitude-dependent and amplitude-independent ranges, respectively. The samples were cooled/heated in a helium atmosphere in an Oxford close-loop cryostat (Oxford Instruments, Abingdon, UK) at a temperature change rate of about 2 K/min.

The type of the martensitic transformation was verified by electrical resistance data. The four-wire alternating current impedance measurements were performed at frequency of 686 Hz and temperature change rate of 2 K/min. The real part of the impedance R was measured using a lock-in amplifier (Stanford Research Systems, Inc., Sunnyvale, CA, USA).

Hydrogen content in variously treated samples was quantified by means of the vacuum hot extraction method. An industrial hydrogen analyser AV-1 (Electronic and Beam Technologies Ltd., St. Petersburg, Russia) was used with mass-spectrometric registration of the time dependence of hydrogen flux from samples heated in vacuum [21]. The analyser was calibrated on certified hydrogen-containing samples of an aluminium alloy with the error of the certified value of hydrogen

concentration of 6%. Hydrogen was extracted from samples in two successive steps at temperatures of 803 K and 1073 K under a working pressure of 10^{-4} Pa.

3. Results

Figure 1 shows the normalized resistance data for the WQ sample. It is seen that the resistance exhibits a sharp change at temperatures near 240 K with narrow temperature hysteresis of about 3 K. Such behaviour is typical for the B2↔R transformation [1,12,22].

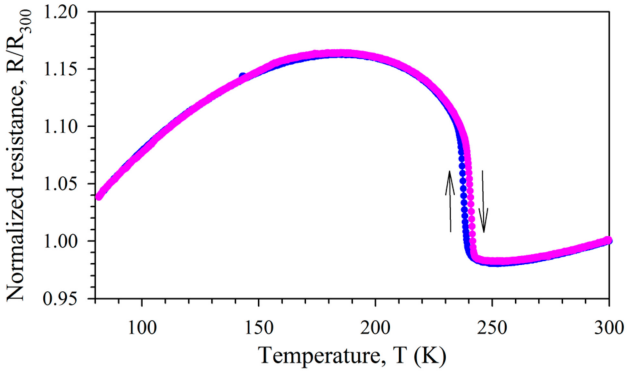

Figure 1. Temperature dependence of resistance for the water-quenched $Ti_{50}Ni_{46.1}Fe_{3.9}$ sample on cooling (blue) and heating (pink). Data are normalized to the resistance values at 300 K.

Results of the hydrogen content evaluation in differently treated samples (WQ and VA) by means of the vacuum hot extraction method are summarized in Table 1. It is seen that hydrogen content varies considerably with heat treatment. The total extracted hydrogen content in the WQ sample is about 5.7 times higher as compared to the VA sample. It is important to note that the effect of the heat treatments is much stronger for the hydrogen fraction extracted at 803 K, because weakly bound states of hydrogen prevail in the WQ sample with increased hydrogen content.

Table 1. Hydrogen extracted from differently treated samples.

Sample	Hydrogen Content, at. ppm		
	Extracted at 803 K	Extracted at 1073 K	Total
WQ	372	79	450
VA	41	38	79

The temperature spectra of the amplitude-independent IF (a) and effective Young's modulus (b) measured in a cooling-heating cycle after the WQ and VA heat treatments are depicted in Figure 2. Two IF maxima are observed after the WQ treatment: (1) a broad maximum at 90 K (on cooling) or 100 K (on heating); and (2) a sharp asymmetric maximum at temperatures of the martensitic transformation, accompanied by a minimum of the effective Young's modulus. The IF of the austenitic phase diminishes after the VA treatment. On the contrary, both the high-temperature IF maximum and the IF of the martensitic phase strongly increase, except the IF at the low-temperature side of the low-temperature IF maximum. As a result of such an effect of the VA treatment, the low-temperature IF maximum transforms into a plateau or a very smooth maximum at temperatures of 150–160 K. Temperature hysteresis of the IF is observed between 80 and 170 K after both heat treatments. E (T) curves measured after the WQ and VA treatments cross at a temperature near 130 K, since E (T) dependence for the WQ sample is weaker in this temperature range.

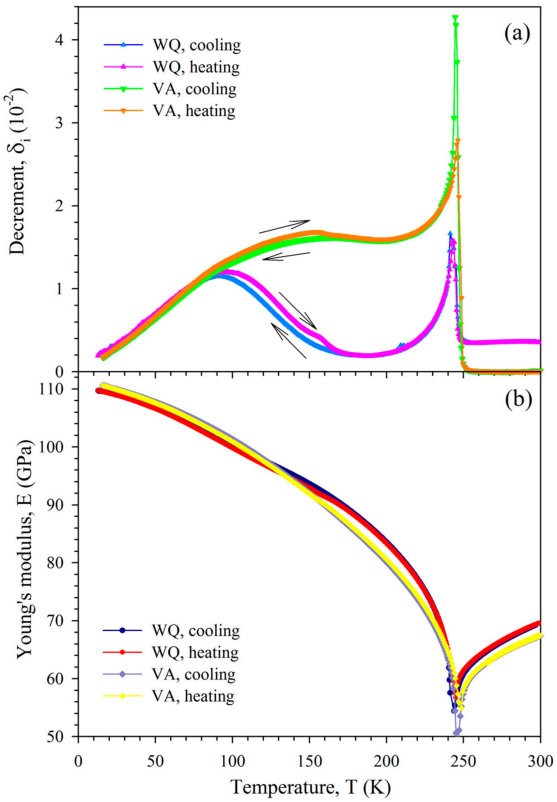

Figure 2. Temperature dependence of the decrement (**a**) and effective Young's modulus (**b**) of the $Ti_{50}Ni_{46.1}Fe_{3.9}$ sample measured in a cooling-heating cycle at strain amplitude of 10^{-6} after water quenching (WQ) or vacuum annealing (VA).

Figure 3 displays the temperature dependence of the temperature coefficient of the Young's modulus, $\alpha_E = (1/E_0) \times (dE/dT)$, calculated for all the curves shown in Figure 2b, with E_0 taken as the Young's modulus value at T = 300 K. One can see that the difference between E (T) curves for WQ and VA samples extends from 80 to 200 K, with lower absolute values of the temperature coefficient of the Young's modulus for the WQ sample. Two different effects can be distinguished in the heating curves: (1) smooth variations between 80 and 200 K, which are reproduced in the cooling curves with some temperature hysteresis; and (2) abrupt changes between 150 and 170 K, which are not observed in the cooling curves.

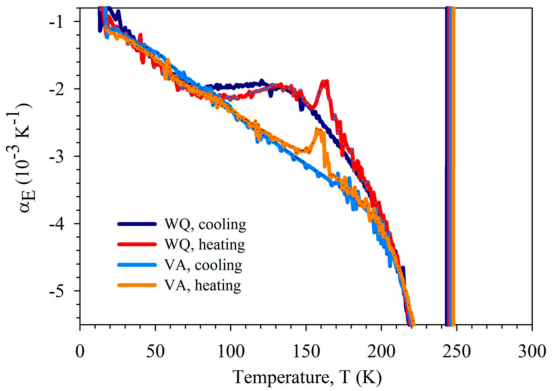

Figure 3. Temperature dependence of the temperature coefficient of the effective Young's modulus of the $Ti_{50}Ni_{46.1}Fe_{3.9}$ sample after water quenching (WQ) or vacuum annealing (VA), derived from the curves shown in Figure 2b.

Figure 4 shows δ_h (a) and $(\Delta E/E)_h$ (b) versus T dependences measured in a cooling-heating cycle for WQ and VA samples. The amplitude-dependent anelasticity (both δ_h and $(\Delta E/E)_h$) in the R phase is strongly promoted by the VA treatment as compared to the WQ treatment, except temperatures below 70 K. For $T < 70$ K the difference between VA and WQ samples is small. Similar to the δ_i (T) dependence, the δ_h and $(\Delta E/E)_h$ versus T dependences for the WQ sample exhibit a maximum, but at a much higher temperatures (140–160 K for δ_h, about 200 K for $(\Delta E/E)_h$). These maxima transform into plateaux or shoulders after the VA treatment. Temperature hysteresis is observed in both characteristics of the amplitude-dependent anelasticity between 140 K and phase transformation temperatures.

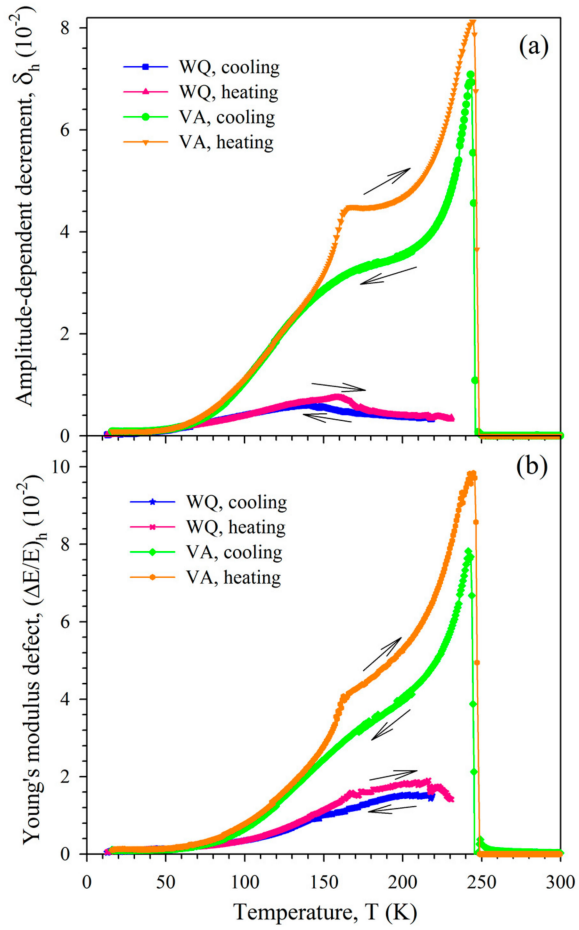

Figure 4. Temperature dependence of the amplitude-dependent components of the decrement (**a**) and Young's modulus defect (**b**) of the $Ti_{50}Ni_{46.1}Fe_{3.9}$ sample measured in a cooling-heating cycle after water quenching (WQ) or vacuum annealing (VA). The dependence is derived from the temperature spectra of the decrement and effective Young's modulus measured at strain amplitudes of 10^{-6} and 5×10^{-5}.

4. Discussion

The anelasticity of the martensitic phases of Ni-Ti-based alloys is usually attributed to the motion of twin boundaries (see, for example, [2,3]). Like other structural defects in solids creating lattice distortions, twin boundaries trap hydrogen atoms [23]. Linear and planar defects trap hydrogen both into core regions and into surrounding stress fields, but separation of these effects is not always possible [24]. Investigations of linear and non-linear components of anelasticity (IF and modulus defect), related respectively to atomic-scale and mesoscopic displacements of linear and planar defects, may enable such separation: the linear (amplitude-independent) anelasticity is sensitive to point

defects situated in the core regions of dislocations/boundaries, whereas non-linear anelasticity is efficient to monitor the changes of point defect concentration in extended point defect atmospheres.

Our data evidence that elastic and anelastic properties of the R phase are very sensitive to variations of hydrogen content. After the conventional heat treatment (WQ) contaminating the alloy with hydrogen, a broad IF maximum is observed at temperatures of 90–100 K (Figure 2a). The high-temperature side of this maximum corresponds to stages in the E (T) dependence with decreasing absolute values of the temperature coefficient (Figure 3). Such behaviour of the effective elastic modulus on heating is conventionally ascribed to a pinning (annealing, recovery) stage (see, for example, [25–27]). Dehydrogenation treatment suppresses strongly the pinning stage provoking the increase of δ_i and transformation of the well-defined low-temperature δ_i (T) maximum into a plateau (or very smooth maximum at higher temperatures of 150–160 K). Similar behaviour of δ_i and E was reported for the B19′ martensitic phase of the $Ni_{50.8}Ti_{49.2}$ alloy [6]. The characteristic pattern of δ_i and E on the high-temperature side of the low-temperature IF maximum on heating/cooling was ascribed to a pinning/depinning stage due to increase/decrease of the hydrogen concentration in the core regions of twin boundaries [6]. The pinning/depinning stage was associated with redistribution of hydrogen between twin boundaries and other structural defects, such as bulk dislocations and/or grain boundaries [6]. As in the case of the $Ni_{50.8}Ti_{49.2}$ alloy [6], only traces of the pinning/depinning stage, caused by a residual hydrogen content, are observed after dehydrogenation treatment of the $Ti_{50}Ni_{46.1}Fe_{3.9}$ alloy (see VA curves in Figures 2–4). Thus, the overall pattern of the δ_i (T) spectra can be qualitatively interpreted as a superposition of the more (high hydrogen content) or less (low hydrogen content) pronounced pinning stage, superimposed on a general IF rise with increasing temperature. In [6], this general trend was associated with a decrease of hydrogen concentration in the core regions of twin boundaries caused by entropy contributions to the binding free energy of a hydrogen atom to a twin boundary. Figure 2a shows that the amplitude-independent IF does not depend on heat treatment at $T < 80$ K. This is an indication that the IF variations for $T < 80$ K is not controlled be the overall hydrogen content (at least for concentrations between 79 and 450 at. ppm).

It should be noted that two different pinning stages are distinguished in the δ_i (T) and E (T) heating curves. The extended smooth stage starting near 80 K is also found on cooling, with certain temperature hysteresis (Figures 2 and 3). This stage is strongly suppressed by dehydrogenation treatment. The abrupt pinning stage at 150–170 K has no correspondence in the cooling curves and is not affected by dehydrogenation treatment. A comparison of linear and non-linear anelastic effects may shed some light on the origin of the stages. The smooth pinning stage is observed only in δ_i (T) and E (T) curves, whereas the abrupt stage can be distinguished, in addition, in δ_h and $(\Delta E/E)_h$ versus T dependences. In Figure 4, the pinning stage is manifested in δ_h (T) curves as a decrease with increasing temperature (heating run for VA sample, cooling and heating runs for WQ sample) or as a shoulder (cooling run for VA sample). Different manifestation of the two pinning stages in the linear and non-linear anelastic properties indicates distinct spatial localization of the hydrogen diffusion paths involved in the redistribution of hydrogen between twin boundaries and other structural defects. During the initial smooth stage, pinning suppresses only short-range mobility of twin boundaries, while their non-linear dynamics on the mesoscopic scale remains unaffected. This evidences that hydrogen diffusion proceeds in the core regions of the defects and, hence, is defect-assisted. The second pinning stage suppresses both short-range and long-range mobility of twins. It is indicative that the second pinning stage is much more extended (30–40 K) in the non-linear anelastic properties as compared to the linear ones. A possible interpretation of the high-temperature pinning stage, affecting both core and extended atmosphere regions of twin boundaries, can involve bulk diffusion of hydrogen. We note here that much faster pipe diffusion of hydrogen along the dislocations, as compared to bulk diffusion, has been reported in Pd [28].

Finally, we note that the present study provides at least two indications that the diffusion mobility of hydrogen interstitials in the R phase is lower than in the B19′ phase: (1) the low-temperature IF maximum and pinning stage in the effective Young's modulus are shifted to higher temperatures in the R phase as compared to the B19′ phase; (2) temperature hysteresis of the IF on the high-temperature

side of the low-temperature IF maximum is observed in the R phase, but not in the B19′ phase. Since hydrogen diffusion over the range of the low-temperature IF maximum is most probably defect-assisted, different structure of twin boundaries may contribute to this distinction between diffusion in the R and B19′ phases.

5. Conclusions

(1) Contamination of the $Ti_{50}Ni_{46.1}Fe_{3.9}$ alloy by hydrogen gives rise to an IF maximum in the R martensitic phase and a complicated pinning stage in the temperature dependence of the effective Young's modulus at temperatures corresponding to the high-temperature side of the IF maximum.

(2) Dehydrogenation heat treatment of the H-contaminated $Ti_{50}Ni_{46.1}Fe_{3.9}$ alloy transforms the IF maximum into a plateau or a smooth maximum caused by a residual hydrogen content.

(3) The IF maximum is associated with a competition of two different temperature-dependent processes affecting the hydrogen concentration in the core regions of twin boundaries, similarly to the non-relaxation IF maximum observed earlier in the B19′ martensitic phase of a $Ni_{50.8}Ti_{49.2}$ alloy.

(4) Amplitude-dependent anelasticity (IF and Young's modulus defect) of the R phase is also very sensitive to hydrogen content, but its maximum values are shifted to higher temperatures as compared to those of the amplitude-independent IF. The temperature dependence of the amplitude-dependent anelasticity is associated with evolution of extended hydrogen atmospheres near twin boundaries.

(5) Diffusion mobility of hydrogen interstitials in the R phase is lower than in the B19′ phase.

Acknowledgments: The work was supported by the Ministry of Education and Science of the Russian Federation, goszadanie No. 3.1421.2017/4.6 and by Spanish Ministerio de Economía y Competitividad, Project MAT2014-56116-C04-01-R. SK acknowledges the support by the Government of Russian Federation (grant No. 074-U01) through the ITMO Fellowship and Professorship Program.

Author Contributions: Konstantin Sapozhnikov, Joan Torrens-Serra and Sergey Kustov conceived, designed and performed the experiments; Eduard Cesari prepared the alloy; Konstantin Sapozhnikov, Joan Torrens-Serra, Eduard Cesari, Jan Van Humbeeck and Sergey Kustov discussed the results; Konstantin Sapozhnikov and Sergey Kustov wrote the paper.

Conflicts of Interest: The authors declare no conflict of interest.

References

1. Otsuka, K.; Ren, X. Physical metallurgy of Ti-Ni-based shape memory alloys. *Prog. Mater. Sci.* **2005**, *50*, 511–678. [CrossRef]
2. Blanter, M.S.; Golovin, I.S.; Neuhäuser, H.; Sinning, H.-R. *Internal Friction in Metallic Materials. A Handbook*; Springer: Berlin/Heidelberg, Germany, 2007.
3. Mazzolai, G. Recent progresses in the understanding of the elastic and anelastic properties of H-free, H-doped and H-contaminated NiTi based alloys. *AIP Adva.* **2011**, *1*, 040701. [CrossRef]
4. Fan, G.; Zhou, Y.; Otsuka, K.; Ren, X.; Nakamura, K.; Ohba, T.; Suzuki, T.; Yoshida, I.; Yin, F. Effects of frequency, composition, hydrogen and twin boundary density on the internal friction of $Ti_{50}Ni_{50-x}Cu_x$ shape memory alloys. *Acta Mater.* **2006**, *54*, 5221–5229. [CrossRef]
5. Fan, G.; Otsuka, K.; Ren, X.; Yin, F. Twofold role of dislocations in the relaxation behavior of Ti-Ni martensite. *Acta Mater.* **2008**, *56*, 632–641. [CrossRef]
6. Sapozhnikov, K.; Torrens-Serra, J.; Cesari, E.; Van Humbeeck, J.; Kustov, S. On the effect of hydrogen on the low-temperature elastic and anelastic properties of Ni-Ti-based alloys. *Materials* **2017**, *10*, 1174. [CrossRef] [PubMed]
7. Zhang, J.; Wang, Y.; Ding, X.; Zhang, Z.; Zhou, Y.; Ren, X.; Wang, D.; Ji, Y.; Song, M.; Otsuka, K.; et al. Spontaneous strain glass to martensite transition in a $Ti_{50}Ni_{44.5}Fe_{5.5}$ strain glass. *Phys. Rev. B* **2011**, *84*, 214201. [CrossRef]

8. Chui, N.Y.; Huang, Y.T. A study of internal friction, electric resistance and shape change in a Ti-Ni-Fe alloy during phase transformation. *Scr. Mater.* **1987**, *21*, 447–452. [CrossRef]
9. Fan, G.; Zhou, Y.; Otsuka, K.; Ren, X. Ultrahigh damping in R-phase state of Ti–Ni–Fe alloy. *Appl. Phys. Lett.* **2006**, *89*, 161902. [CrossRef]
10. Yoshida, I.; Monma, D.; Ono, T. Damping characteristics of $Ti_{50}Ni_{47}Fe_3$ alloy. *J. Alloys Compd.* **2008**, *448*, 349–354. [CrossRef]
11. Fan, G.; Zhou, Y.; Otsuka, K.; Ren, X. Comparison of the two relaxation peaks in the $Ti_{50}Ni_{48}Fe_2$ alloy. *Mater. Sci. Eng. A* **2009**, *521–522*, 178–181. [CrossRef]
12. Wang, D.; Zhang, Z.; Zhang, J.; Zhou, Y.; Wang, Y.; Ding, X.; Wang, Y.; Ren, X. Strain glass in Fe-doped Ti–Ni. *Acta Mater.* **2010**, *58*, 6206–6215. [CrossRef]
13. Zuo, S.; Jin, M.; Chen, D.; Jin, X. Origin of the anelastic behavior in $Ti_{50}Ni_{44}Fe_6$ alloy. *Scr. Mater.* **2015**, *108*, 113–116. [CrossRef]
14. Chang, S.H.; Chien, C.; Wu, S.K. Damping characteristics of the inherent and intrinsic internal friction of $Ti_{50}Ni_{50-x}Fe_x$ (x = 2, 3, and 4) shape memory alloys. *Mater. Trans.* **2016**, *57*, 351–356. [CrossRef]
15. Zhang, J.; Xue, D.; Cai, X.; Ding, X.; Ren, X.; Sun, J. Dislocation induced strain glass in $Ti_{50}Ni_{45}Fe_5$ alloy. *Acta Mater.* **2016**, *120*, 130–137. [CrossRef]
16. Yokoyama, K.; Tomita, M.; Sakai, J. Hydrogen embrittlement behavior induced by dynamic martensite transformation of Ni-Ti superelastic alloy. *Acta Mater.* **2009**, *57*, 1875–1885. [CrossRef]
17. Saito, T.; Yokoyama, T.; Takasaki, A. Hydrogenation of TiNi shape memory alloy produced by mechanical alloying. *J. Alloys Compd.* **2011**, *509* (Suppl. 2), S779–S781. [CrossRef]
18. Ribeiro, R.M.; Lemus, L.F.; dos Santos, D.S. Hydrogen absorption study of Ti-based alloys performed by melt-spinning. *Mater. Res.* **2013**, *16*, 679–682. [CrossRef]
19. Robinson, W.H.; Edgar, A. The piezoelectric method of determining mechanical damping at frequencies of 30 to 200 kHz. *IEEE Trans. Sonics Ultrason.* **1974**, *21*, 98–105. [CrossRef]
20. Kustov, S.; Golyandin, S.; Ichino, A.; Gremaud, G. A new design of automated piezoelectric composite oscillator technique. *Mater. Sci. Eng. A* **2006**, *442*, 532–537. [CrossRef]
21. Polyanskiy, A.M.; Polyanskiy, V.A.; Yakovlev, Y.A. Experimental determination of parameters of multichannel hydrogen diffusion in solid probe. *Int. J. Hydrogen Energy* **2014**, *39*, 17381–17390. [CrossRef]
22. Choi, M.S.; Fukuda, T.; Kakeshita, T. Anomalies in resistivity, magnetic susceptibility and specific heat in iron-doped Ti-Ni shape memory alloys. *Scr. Mater.* **2005**, *53*, 869–873. [CrossRef]
23. So, K.H.; Kim, J.S.; Chun, Y.S.; Park, K.T.; Lee, Y.K.; Lee, C.S. Hydrogen delayed fracture properties and internal hydrogen behavior of a Fe-18Mn-1.5Al-0.6C TWIP steel. *ISIJ Int.* **2009**, *49*, 1952–1959. [CrossRef]
24. Myers, S.M.; Baskes, M.I.; Birnbaum, H.K.; Corbett, J.W.; DeLeo, G.G.; Estreicher, S.K.; Haller, E.E.; Jena, P.; Johnson, N.M.; Kirchheim, R.; et al. Hydrogen interactions with defects in crystalline solids. *Rev. Mod. Phys.* **1992**, *64*, 559. [CrossRef]
25. Thompson, D.O.; Pare, V.K. Effect of fast neutron bombardment at various temperatures upon the Young's modulus and internal friction of copper. *J. Appl. Phys.* **1960**, *31*, 528–535. [CrossRef]
26. Magalas, L.B.; Moser, P. Internal friction in cold worked iron. *J. Phys. Coll.* **1981**, *42*, C5-97–C5-102. [CrossRef]
27. Takamura, S.; Kobiyama, M. Dislocation pinning in Al and Ag alloys after low-temperature deformation. *Phys. Stat. Sol. A* **1986**, *95*, 165–172. [CrossRef]
28. Kirchheim, R. Interaction of hydrogen with dislocations in palladium—I. Activity and diffusivity and their phenomenological interpretation. *Acta Metall.* **1981**, *29*, 835–843. [CrossRef]